Larrañaga-Valsero, B., Smith, R. A., Tayong Boumda, R., Fernández-López, A., & Güemes, A. (2016). Wrinkle characterisation from ultrasonic scans of composites. 508-521. Paper presented at 55th Annual Conference of the British Institute of Non-Destructive Testing, NDT 2016, Nottingham, United Kingdom.

Early version, also known as pre-print

Link to publication record in Explore Bristol Research
PDF-document

University of Bristol - Explore Bristol Research
General rights

Wrinkle characterisation from Ultrasonic Scans of Composites

Beatriz Larrañaga-Valsero[1], Robert A. Smith[2], Rostand B. Tayong[2],

Antonio Fernández-López[1] and Alfredo Güemes[1].

[1]Department of Materials and Aerospace Production. Polytechnic University of Madrid, SPAIN.

beatriz.larranaga.valsero@aero.upm.es; antonio.fernandez.lopez@upm.es, alfredo.guemes@upm.es

[2] Department of Mechanical Engineering, University of Bristol, BS8 1TR, UK

e-mail: Robert.smith@bristol.ac.uk; rt14172@bristol.ac.uk

Abstract

Wrinkles (out-of-plane waviness) are, unfortunately, a common phenomenon during composite manufacture and have a significant influence on the mechanical performance. While the aviation industry tries to reduce the thickness of composites for weight reasons, more plies are added to the design in order to mitigate the risk of undetected wrinkles and ensure robust mechanical properties of structures. The aim of this work is to detect and characterise out of plane wrinkles in complex glass-carbon structures using ultrasonic non-destructive tests. The parts to be inspected are made of epoxy resin reinforced with unidirectional carbon fibre and woven glass fibre. In order to determine the ideal probe frequency and bandwidth with which the inspections must be made, the resonant frequency of the plies was determined using a MATLAB-based analytical model. The parts were then inspected using full-matrix capture (FMC) and the total focusing method (TFM) as well as a commercial phased-array instrument providing data that can be inverted to give out-of-plane ply direction. Finally, the amplitude of the wrinkle was measured visually on the samples and compared with the ultrasonic measurements to determine the accuracy of the proposed method.

1. Introduction

The use of composites by increasingly diverse industries and the optimization of the designs has caused the design of parts with complex geometries and lay-ups. For instance, in order to withstand the large bending moments at the root of large turbine blades, very thick carbon and glass fibre laminates are used. Wrinkles are common defects in such parts; they affect the mechanical properties[1] and force the designers to add even more plies to mitigate the potential decrease in the strength. Hence, it is important to be able to fully characterise the increasingly complex parts manufactured by the industry.

Although Micro-focus X-Ray Computed Tomography (Micro-CT) is considered to be the reference in terms of detectability of fibre waviness, it is expensive and is not a practical technique for field inspections or for large components[2]. Manufacturers and end users are interested on finding a method to characterise the defects in composite parts with the level of detail provided by CT but with more practical techniques. Some research has been done trying to detect in-plane waviness in composites using eddy-current imaging. Experiments with cross-ply laminates (0 and 90 degree plies only) showed that the shape and size of the surface waviness could be estimated with high accuracy, whereas the size

of the sub-surface waviness was underestimated. However, the proposed eddy-current imaging method can detect in-plane waviness only when the direction of the long sides of the driver coil corresponds to that of the carbon fibre plies with waviness[3-4]. Ultrasonic techniques are commonly used for composite material inspection. Pain and Drinkwater[5] showed that ultrasonic array scattering data could be used for the detection of out-of-plane wrinkles in a thick carbon-fibre sample. Ultrasound can image, measure and map the ply lay-up of composite materials, through the 3D full-waveform scans of the samples[6-7]. In-plane waviness can be characterised through C-Scan slices and out-of-plane wrinkles can be characterised through B-Scan slices[8]. Smith et al[9] proved that the instantaneous phase of the 3D full-waveform scan tracks the depths of the resin layers and allows out-of-plane wrinkles to be mapped within the structure. Of particular significance is that the instantaneous phase increases by 2π radians per ply for the fundamental resonance and 4π radians for the second-harmonic resonance.

Even though ultrasound is the most developed NDT technique for 3D characterisation of composites, most of the work has been demonstrated on thin monolithic mono-material structures. The work presented in this paper is focused on the detection of out–of-plane wrinkles in thick carbon/glass fibre composites using ultrasonic techniques that have proved to be effective for detecting wrinkles in mono-fibre composites. The methods are then applied using two data acquisition types: full-matrix capture (FMC) with total focusing method (TFM) reconstruction and phased-array ultrasound. Phased-array is a commercial technique that is effective for detecting impact damage[10] in composites.

2. Experimental samples

Three test samples (J, B, C) (see Figure 1) with two different wrinkles and two lay-ups are used for the experiments. The parts to be inspected are made of two materials: epoxy resin reinforced with either unidirectional carbon fibre (nominal ply thickness 0.6 mm) or woven glass fibre (nominal woven-ply thickness 0.44 mm). Specimen J is mainly carbon fibre with just two woven glass-fibre layers, the first and last plies. Specimens B and C have one woven glass ply followed by five carbon plies (one woven glass ply every six plies). The nominal fibre volume fraction and nominal inter-ply resin-layer thickness are not known but 60% and 0.01 mm respectively were used in the model. All the wrinkles affect the full width of the parts and the wrinkle is located in the middle of the sample.

Figure 1: Samples J (left), B (middle) and C (right)

The samples were designed and manufactured to have a reference ply in the middle, which has a known maximum wrinkle amplitude. In the manufacture of each laminate the shape of the reference layer was achieved by using male tools made of aluminium with a cosine geometry (see Figure 2). Half of the plies were stacked on the male tool and cured. The remaining layers were stacked on the cured half-laminate with the tool removed, forced into the concave wrinkle and cured in a hot-plate press in order to obtain a controlled thickness. The stiffness of the carbon fibres meant that the severity of the wrinkle in the secondary half-laminate was not as great as the wrinkle formed on the tool, because it was difficult to get the pre-preg to adapt to the shape of the previously cured half-

laminate. Specimen C has a thick resin-rich layer as a result the resistance of the fibres to bend. A void appeared half-way through in the wrinkle region in this thick resin layer.
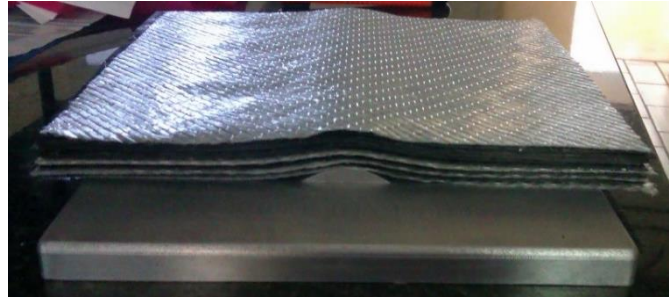

Figure 2: Aluminium tool used during the manufacture of the specimens with half of the plies stacked on it before curing. The effect where the layers do not conform to the geometry of the tool can be seen clearly.

Although wrinkles significantly affect the mechanical performance of composite parts, different parameters have been used in the past to characterise them: maximum amplitude (H) [11], severity[12] or maximum angle. Xie et al[13] have shown that the maximum wrinkle angle has a dominant influence on compressive failure stress, compared with the wavelength or the amplitude. The unusual geometry of wrinkles in samples J, B and C make it necessary to find a compromise between the parameters that are used in the literature and the parameters that are used by the industry. Defining the 'severity' of the wrinkle as 2A/L is consistent with the industry and the literature but L is defined here as a wrinkle wavelength (see Figure *3*Figure 3). In this paper the feature angle, θ, is measured with a protractor for the slope of the tangent to the curve at the point where it intersect with the imaginary parallel line at a distance A from the flat part of the wrinkle. . Even though more consistent ways to obtain an angle measurement have been developed[14], this method has been chosen for its simplicity and as a compromise between the scientific literature and industrial usage. The values measured for the three specimens are given in Table 1 and should be interpreted with reference to Figure 3.
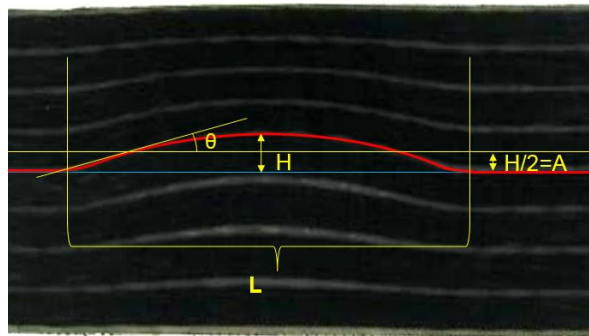

Figure 3: Wrinkle parameters

Table 1: Characteristics of the Test Specimens

Specimen	J	B	C
Thickness	23 mm	27 mm	26 mm
Number of Plies	42	49	49
Wrinkle Maximum height H	3 mm	3 mm	6 mm
Wrinkle "Severity" 2A/L	0.06	0.06	0.18
Wrinkle Angle θ	8.5°	8.5°	24°

3. Analytical modelling for probe optimisation

In order to determine the ideal probe frequency and bandwidth with which the ultrasonic inspections should be made, it is necessary to first determine the resonant frequency of the plies. A one-dimensional normal-incidence analytical model developed by Smith[15 - 16] had been coded in Matlab and was used to simulate all the composite laminates. The model uses the thickness, density and compression modulus for each layer to calculate the laminate response for a normal-incidence plane wave. A wrinkle can be modelled, despite this being a one-dimensional model, by gradually changing the layer properties to describe the shape of the wrinkle.

18-ply laminates were simulated initially in both e-glass and carbon fibre. The reflection-coefficient frequency spectrum of the non-wrinkled laminate allows the determination of the resonant frequencies corresponding to a 0.6 mm carbon-fibre ply and a 0.44 mm glass-fibre ply (Figure 4).
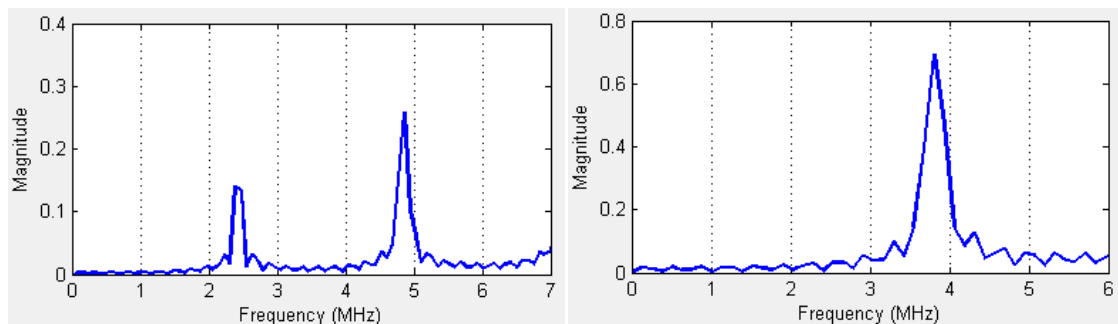

Figure 4: Reflection coefficient of an 18 layers carbon fibre laminate with a 0.6 mm ply spacing (left) and of an 18 layers e-glass fibre laminate with a 0.44 mm ply spacing (right).

The model gave the fundamental resonant frequency, F_{R1}, for a 0.6 mm ply spacing in a carbon fibre composite as 2.3 MHz, whilst the second-harmonic resonance, F_{R2}, is at 4.7 MHz. The fundamental resonant frequency for a 0.44 mm ply spacing in glass-fibre composite is 3.8 MHz (F_{R1}). This disparity in frequencies makes it difficult to resonate all layers with one pulse, which would enable a layer-by-layer mapping of the complete laminate. However, it may be possible, with a broad-band transducer, to include all these frequencies in the pulse bandwidth.

In addition, the ply spacing decreases at the wrinkle, where the layers are compacted, causing an increase in the resonant frequency which then varies within the wrinkle region. The bigger the wrinkle amplitude, the higher is the maximum resonant frequency at the position of maximum deviation. In an 18-ply carbon fibre laminate, a 3 mm amplitude wrinkle causes the ply thickness to decrease from 0.6 mm down to 0.433 mm and an increase in the resonant frequency from 2.3 MHz up to 3.0 MHz.

There are two probe options for including the carbon-fibre ply-resonance range as well as the glass-fibre ply-resonance frequency of 3.8 MHz – see Figure 5. A 2.25 MHz broad-band probe with a 2.25 MHz pulse-echo bandwidth would include all the fundamental resonant frequencies of the carbon plies whilst being centred on the fundamental resonance of the unwrinkled carbon plies. Alternatively, a 5 MHz narrow-band probe with a 2.5 MHz pulse-echo bandwidth would be centred on the second harmonic of the carbon plies and include the fundamental glass-ply resonance and the second-harmonic frequency range of the carbon plies (4.7 to 6.0 MHz). The simulated responses of a 36 carbon-ply laminate with a 3 mm amplitude wrinkle in the middle are shown in Figure 5 for both of these probe options.
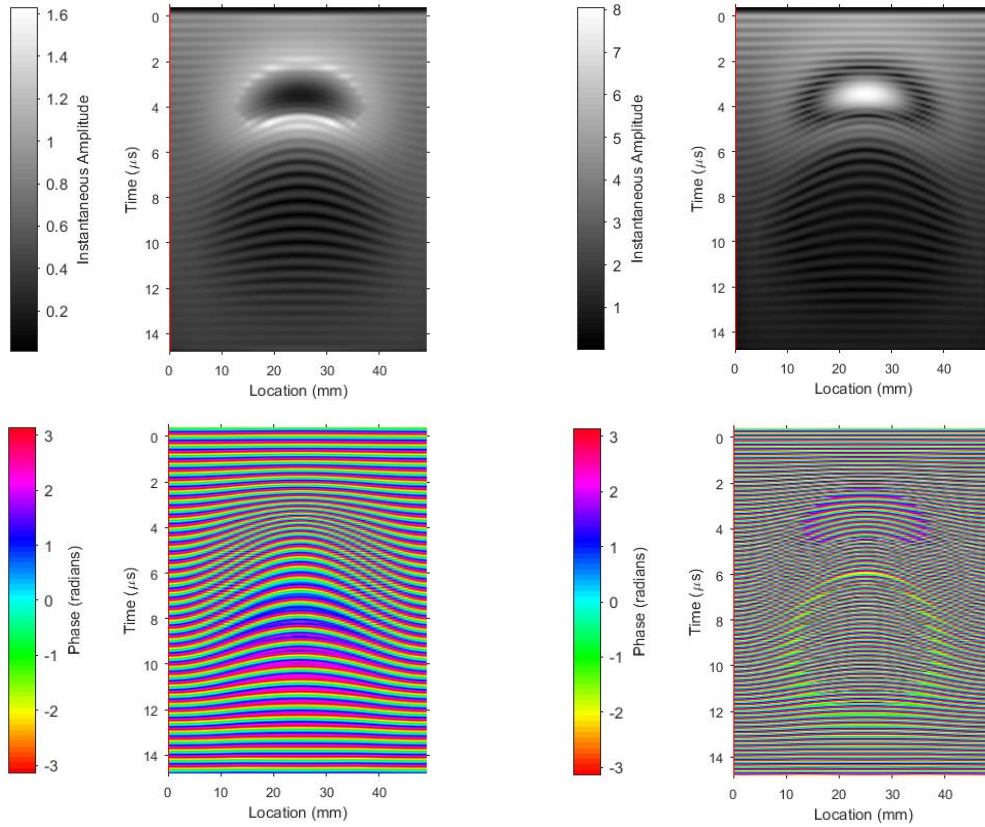
4

Figure 5. Simulated instantaneous amplitude (top) and phase (bottom) for 36 carbon-fibre plies of thickness 0.59 mm with 0.01 mm resin layers and a 3mm amplitude wrinkle at the centre. 2.25 MHz centre frequency and 2.25 MHz bandwidth (left) and 5 MHz centre frequency and 2.5 MHz bandwidth (right).

It is clear from the phase images that the 2.25 MHz probe excites the fundamental ply resonance and that the whole range of ply thicknesses through the wrinkle are within the bandwidth of the probe. The 5 MHz probe excites the second harmonic except in the zone above the wrinkle where the plies become thinner and the fundamental resonant frequency increases until it dominates over the second harmonic. Both probe options appear to track the wrinkle accurately in both amplitude and phase, but interpretation is considerably easier for the 2.25 MHz probe.

The mixed carbon/glass laminates have also been modelled – see Figure 6 for the 2.25 MHz simulations. These responses are much more complicated because the glass-fibre woven plies are highly reflective and dominate the response. The result is a complicated interference pattern of primary reflections and multiple reflections from the glass plies, seen in both the amplitude and phase-response images. The multiple reflections may be exaggerated in the model, which assumes plane waves and infinite flat plies. The real laminate would have angled plies in the wrinkle region and multiple reflections would consequently be at significantly lower amplitudes.
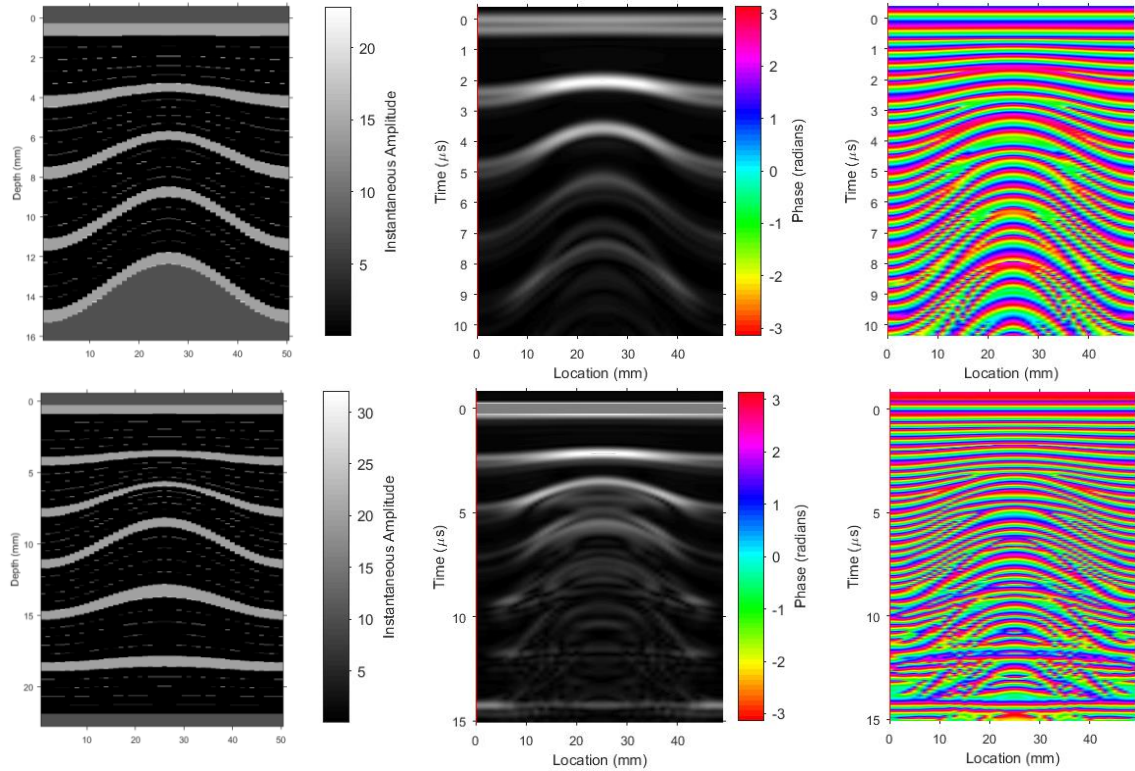
5

Figure 6. Simulated responses using a 2.25 MHz centre frequency and 2.25 MHz bandwidth for carbon-fibre plies of thickness 0.59 mm and 0.01 mm resin layers but with a 0.44 mm thick glass-fibre ply every 6th ply; 25 plies with a 3 mm amplitude wrinkle at the back surface (top) and 36 plies with a 3 mm wrinkle in the middle (bottom). Lay-up diagram (left), instantaneous amplitude (middle) and instantaneous phase (right).

4. Experimental results

Two inspection methods were considered in the experimental part of the project. The first is full-matrix capture (FMC)[17] with reconstruction of B-scan slices using the total focusing method (TFM)[18]. This was accomplished using a 2.5 MHz or 5 MHz array probe connected to a Diagnostic Sonar 'FIToolbox' array controller working with the proprietary Matlab-based BRAIN software developed at the University of Bristol [19]. The sample frequency used was 25 MHz.

4.1 Full-matrix capture with total-focusing method

4.1.1 Results with a 2.5 MHz array probe
The specimen J was first inspected with the 2.5 MHz probe from its convex side (Figure 7) and from its concave side (Figure 8) mounted directly on the surface of the sample, with no stand-off. Both inspections allow the detection of the wrinkle and a strong back echo appears. The instantaneous amplitude shows the waviness, but it is in the instantaneous phase where the wrinkle can be detected and fully characterised. All the required dimensional parameters of the wrinkle seem to be measurable, as expected from the simulations and for sample J, being mainly carbon fibre. In the non-wrinkle area, all the plies can be tracked through the thickness until the amplitude decays significantly whereas, in the wrinkle-area, the frequency increase caused by the compaction of the plies does not allow every ply to be tracked. This suggests that the bandwidth of the probe is insufficient for this amplitude of wrinkle.
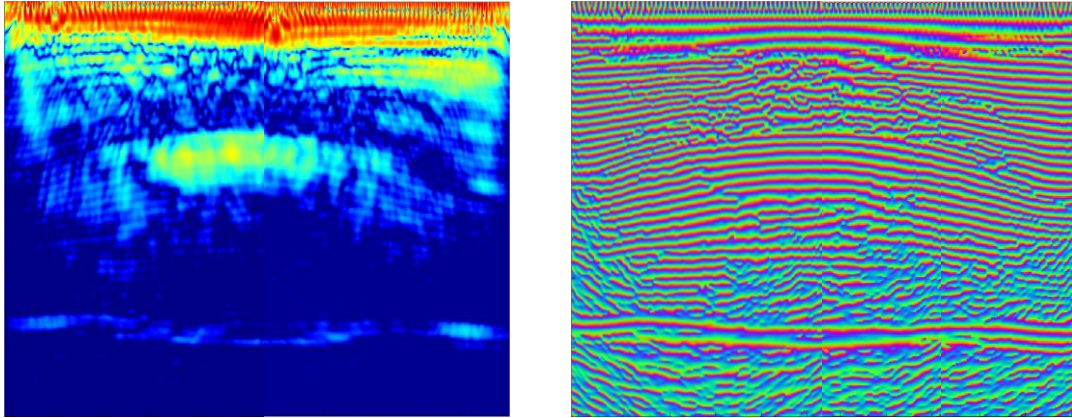
6

Figure 7: Instantaneous Amplitude (left) and Instantaneous Phase (right) at 2.5MHz of the specimen J from the convex side of the wrinkle.
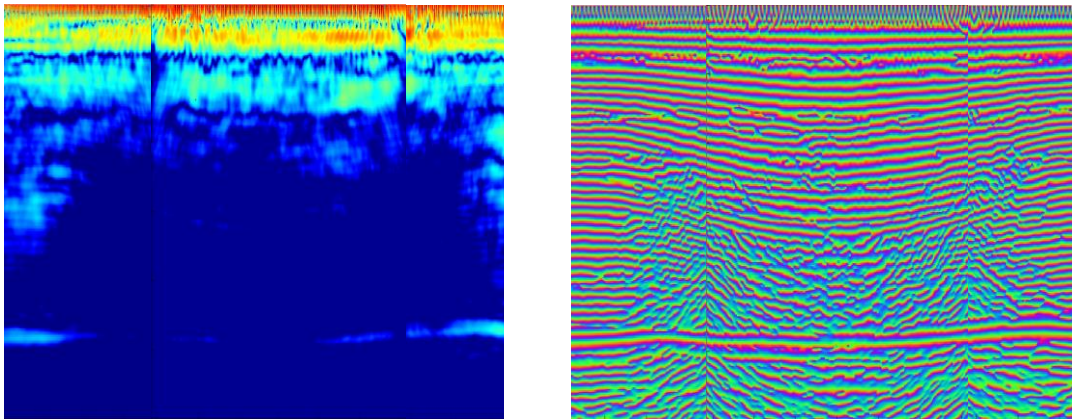

Figure 8: Instantaneous Amplitude (above) and Instantaneous Phase (below) at 2.5MHz of the specimen J from the concave side of the wrinkle.

Specimen B was then inspected with the 2.5 MHz probe, from both sides with the same configuration (Figure 9 and Figure 10). This only allows visualisation of the wrinkle from the convex side (Figure 9) where an apparent variation appears in the phase that can be identified as the back-wall echo at some areas of the wrinkled and non-wrinkled zone.
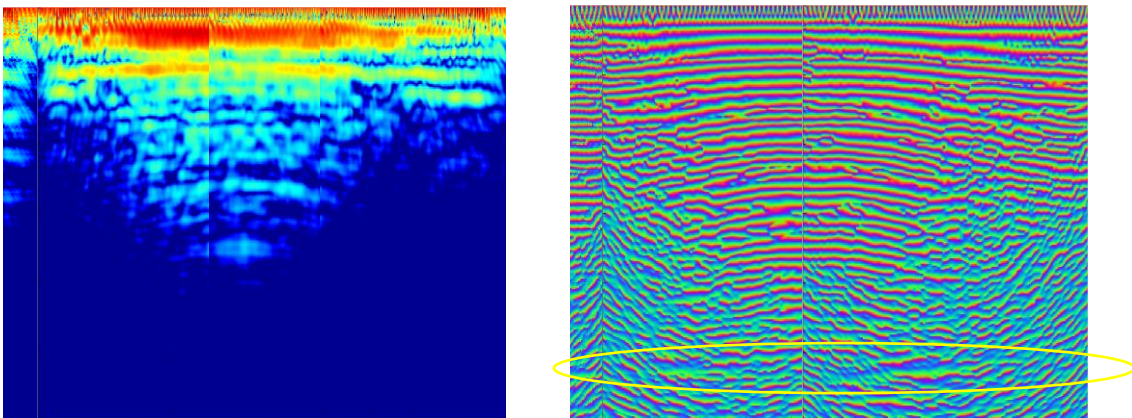

Figure 9: Instantaneous Amplitude (left) and Instantaneous Phase (right) at 2.5MHz of the specimen B from the convex side of the wrinkle. : The potential back-wall echo is circled in yellow.
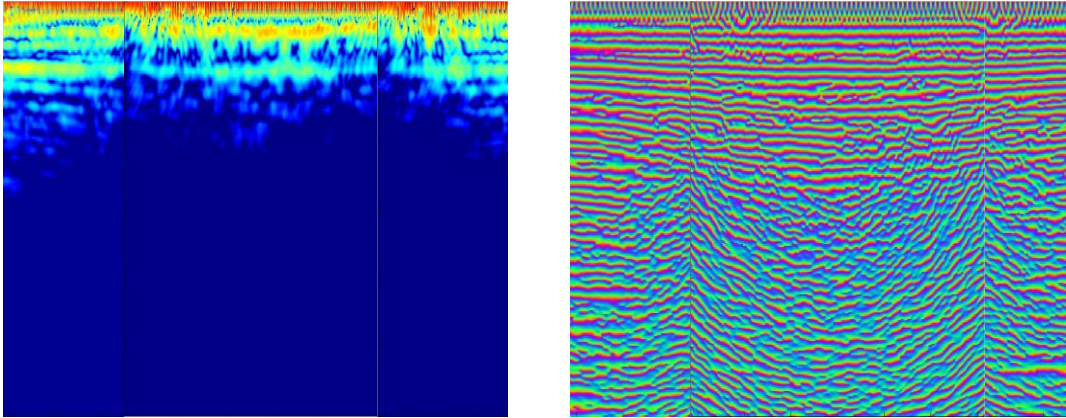
7

Figure 10: Instantaneous Amplitude (left) and Instantaneous Phase (right) at 2.5MHz of the specimen B from the concave side of the wrinkle.

Specimen C was then inspected with the 2.5 MHz probe, from both sides with the same configuration. (Figure 11 and Figure 12) This allows visualisation of the wrinkle from the convex side (Figure 11). The instantaneous amplitude shows some waviness and some strong echoes at the centre of the wrinkle. In the instantaneous phase the wrinkle can be fully characterised. No echo appears that could be identified as the back-wall echo. The inspection from the concave side (Figure 12) doesn't really allow the detection of the wrinkle, because even if a wrinkle is perceive, there is no a clear line to follow.
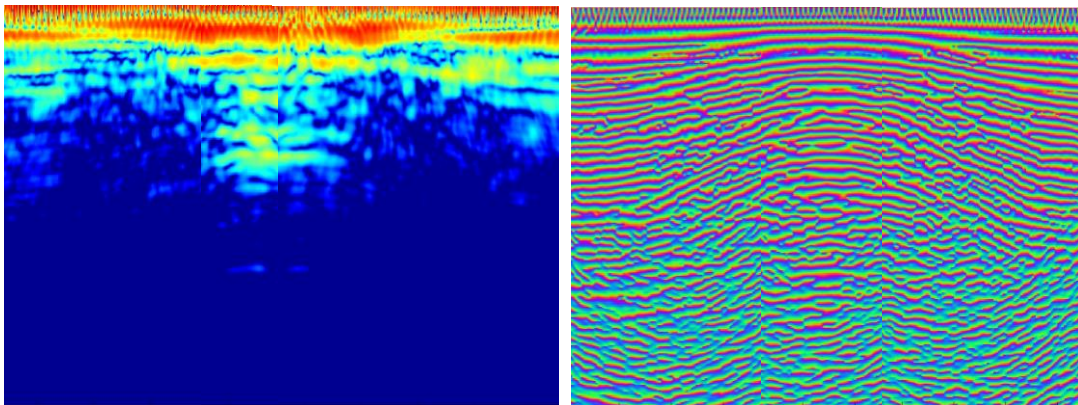

Figure 11: Instantaneous Amplitude (left) and Instantaneous Phase (right) at 2.5MHz of the specimen C from the convex side of the wrinkle.
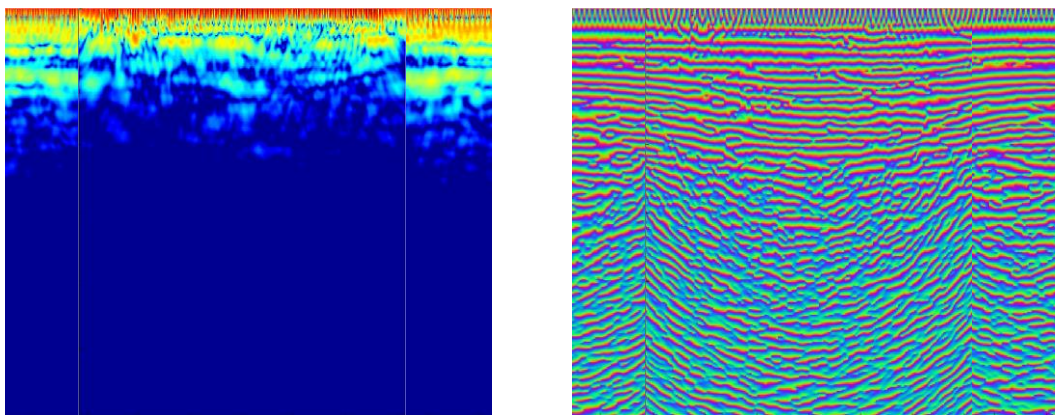

Figure 12: Instantaneous Amplitude (above) and Instantaneous Phase (below) at 2.5MHz of the specimen C from the concave side of the wrinkle.

8

The measurements of the parameters were achieved with an electronic rule or protractor on the B-Scan slices reconstructed with the TFM. The results obtained are summarised in Table 2 and should be interpreted with reference to Figure 3. None of the inspections showed any further defects in the non-wrinkled area.

Table 2: Comparison between the actual parameters of the parts and those obtained from the convex side of the samples by the inspection with a TFM 2.5 MHz probe.

Specimen	J		B		C	
	Expected	Measured	Expected	Measured	Expected	measured
Wrinkle Maximum height H	3 mm	3.2 mm	3 mm	3.6 mm	6 mm	6.5 mm
Wrinkle "Severity" 2A/L	0.06	0.065	0.06	0.075	0.18	0.15
Wrinkle Angle θ	8.5°	8.5°	8.5°	9°	24°	22°

4.1.2 Results with a 5MHz Array probe
Specimen J was inspected with the 5 MHz probe mounted directly on the convex surface of the sample, with no stand-off - see Figure 13. The back-wall echo appears on both instantaneous phase and amplitude images. All the required dimensional parameters of the wrinkle seem to be measurable
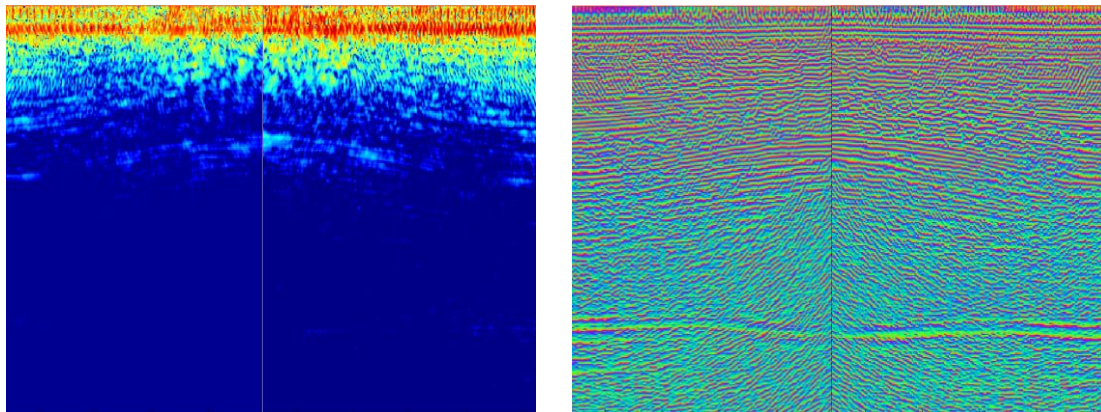

Figure 13: Instantaneous Amplitude (left) and Instantaneous Phase (right) at 5MHz for specimen J.

Specimen B was then inspected with the same 5 MHz probe and configuration (*Figure 14*). The back-wall echo still appears in the instantaneous-phase image but the wrinkle maximum height (H) and the angle θ are not measurable because, even if a wrinkle is evident in the image, there is no a clear ply-interface line to follow. Only a method able to measure the angle of the wrinkle at any point[2] will be effective to characterise the wrinkles in this case.
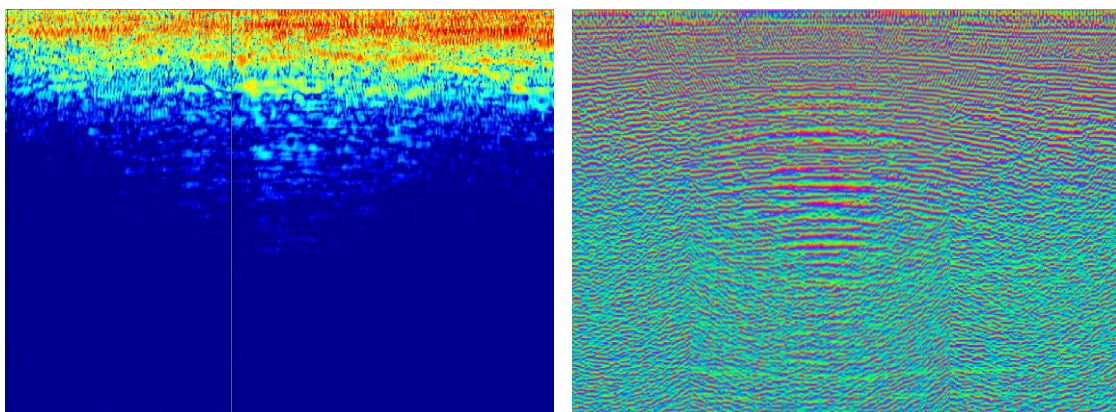

Figure 14: Instantaneous Amplitude (left) and Instantaneous Phase (right) at 5MHz for specimen B

9

Specimen C was also inspected with the 5 MHz probe (Figure 15). The instantaneous amplitude still shows some waviness in the higher zone of the wrinkle. The back-wall echo does not appear in either of the amplitude or phase images and the height of the wrinkle, H, is not measurable because of the impossibility of following the ply lines.
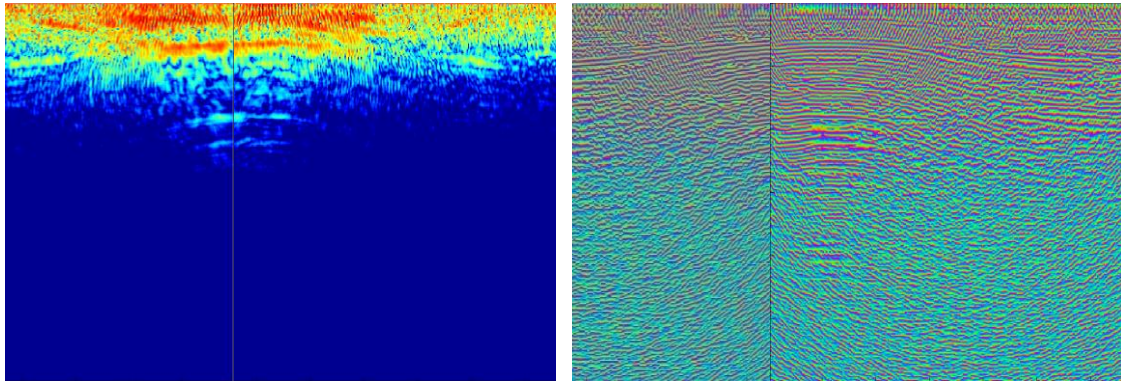

Figure 15: Instantaneous Amplitude (left) and Instantaneous Phase (right) at 5MHz for specimen C

At 5 MHz, the instantaneous phase increases by 4π radians per ply, as expected for the second-harmonic resonance. Only the first half of the specimen seems to be clearly represented in the images - beyond this there are too many confusing interferences to visualise any clear pattern. The dampening effect of the glass-fibre layers in samples B and C prevents proper inspection of the entire thickness and only weak back-wall echoes are obtained in this case. Reducing the pixel size by increasing the digital waveform sampling frequency would also help to produce clearer images. However, a simpler solution would be to use a 2.25 MHz probe with a wide bandwidth and visualise the fundamental resonance rather than the second harmonic. In this case, the phase would only increase by 2π radians per ply and the plies would be clearer in the phase image without having to increase the sampling frequency. An additional benefit would be that the attenuation would be reduced and deeper penetration of the ultrasound would result.

The measurements of the parameters were done with an electronic rule or protractor on the B-Scan slices reconstructed with the TFM. The results obtained are summarised in Table 3 and should be interpreted with reference to Figure 3. As predicted by the simulations, interpretation was easier for the 2.5 MHz.

Table 3: Comparison between the actual parameters of the parts and those obtained from the convex side of the samples by the inspection with a TFM 5 MHz probe.

Specimen	J		B		C	
	Expected	Measured	Expected	Measured	Expected	Measured
Wrinkle Maximum height H	3 mm	3.5 mm	3 mm	-	6 mm	-
Wrinkle "Severity" 2A/L	0.06	0.08	0.06	-	0.18	-
Wrinkle Angle θ	8.5°	10°	8.5°	-	24°	-

It is possible to characterise the wrinkles with a reasonable precision using FMC/ TFM, the instantaneous phase of the received signal and an appropriate inspection frequency (in this case 2.5 MHz). Although it is possible to characterise the wrinkles with a representative angle, θ, it is not possible to differentiate the area affected by the wrinkle, which might be significant for mechanical strength[13]. One of the major difficulties encountered in defining the wrinkle accurately is to follow the line of maximum amplitude of the wrinkle (the reference layer). In many specimens only half of the part

10

presents a clear image. This would make it impossible to measure the wrinkle if the reference layer was in the second half.

An important point that has not been considered in this work is the effect of Fibre Volume Fraction on velocity. The Fibre Volume Fraction varies considerably inside a wrinkle and this effect can distort the measurement of the amplitude of the wrinkles particularly in the glass specimens [15]. It will be worthwhile to analyse this effect in future work.

4.2 Phased-array technology

FMC and TFM may not be needed to fully characterise the wrinkles. Phase-array technology or a raster-scanned single-element probe may also be adequate.

Specimen J was inspected with the 5 MHz probe mounted directly on the surface of the sample using an Olympus OmniScan instrument (Figure 16). The back-wall echo does appear on both angle and amplitude images. In this case, the OmniScan does not provide the instantaneous phase of the wave, so the signal was processed in Matlab to obtain a coarse 'instantaneous phase' which just shows whether the real waveform (RF) is positive (black) or negative (white) – ie black for a phase ϕ of $-\pi/2 < \phi < \pi/2$ and white for a phase $\pi/2 < \phi < 3\pi/2$. The top surface of the sample is hidden in the dead zone of the probe, preventing proper characterization of the wrinkle.
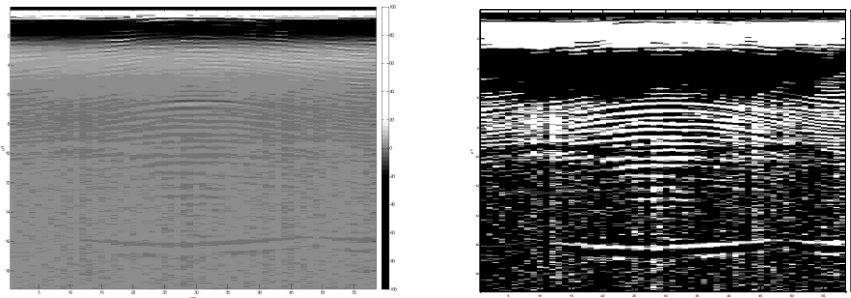

Figure 16: RF signal (left) and "Instantaneous Phase" (right) at 5MHz of the specimen J. The near-surface dead zone of the probe is large (9 mm) and does not allow measurement of the wrinkle. The ultrasonic beam was focused at 15 mm depth.

In order to avoid the effect of the dead zone, a stand-off was placed between the probe and the sample. Using a stand-off is a common practice with ultrasonic probes in order to force the dead zone to occur before the front-surface reflection, so that it does not interfere with the echoes of the sample. The thickness of the stand-off is a very important parameter and is governed by two criteria. The first criterion is that the time-of-flight through the stand-off must be greater than through the sample because otherwise the interface between the stand-off and the sample creates a strong multiple-reflection echo, which would be superimposed on the actual defect echoes. The second criterion is that the focal depth should be half-way through the sample. However, the ultrasonic beam can only be focused in the 'equivalent' near-field of the ultrasonic beam from a flat transducer of the same size. This equivalent near-field location is nearer the front surface if the probe is mounted on the stand-off, so a larger transducer is then required to force a deeper near-field distance. A 20 mm thick Rexolite stand-off was used, which does not meet the first criterion, but does meet the second.

Specimen J was inspected with the 5 MHz probe with a 20 mm thick Rexolite stand-off and Omniscan (Figure 17). The back-wall echo (marked 'B') does appear on the amplitude image but should not be mistaken for the second multiple echo from the stand-off (marked '2'), which appears just after the back-wall echo and dominates in the instantaneous amplitude image. In the RF signal and the instantaneous amplitude, the

11

back echo is stronger whereas in the instantaneous angle the second multiple of the stand-off is stronger. Specimen B and C were then inspected with the 5 MHz probe (Figure 18 and Figure 19 respectively). The back-wall echo does not appear on either the phase or the instantaneous amplitude, probably because it coincides with the second multiple of the stand-off.
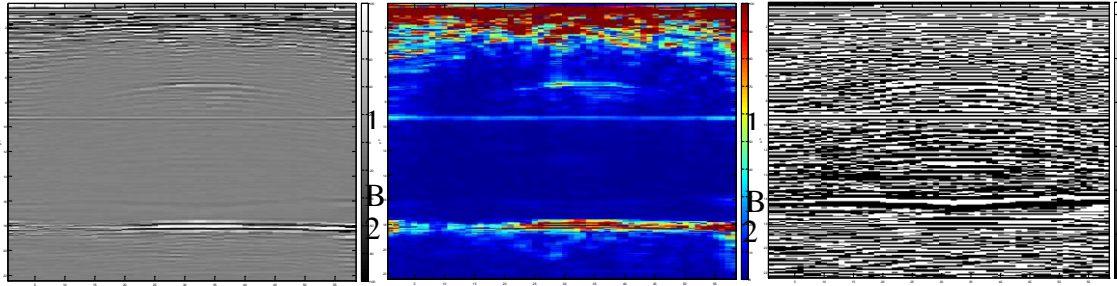

Figure 17: Specimen J 5 MHz Omniscan RF signal (left), Instantaneous Amplitude (centre) and "Instantaneous phase" (right) at 5MHz of the specimen A and a 20 mm thick Rexolite stand-off. The back-wall echo is labelled 'B' and the first and second multiple echoes of the stand-off are labelled '1' and '2' respectively.
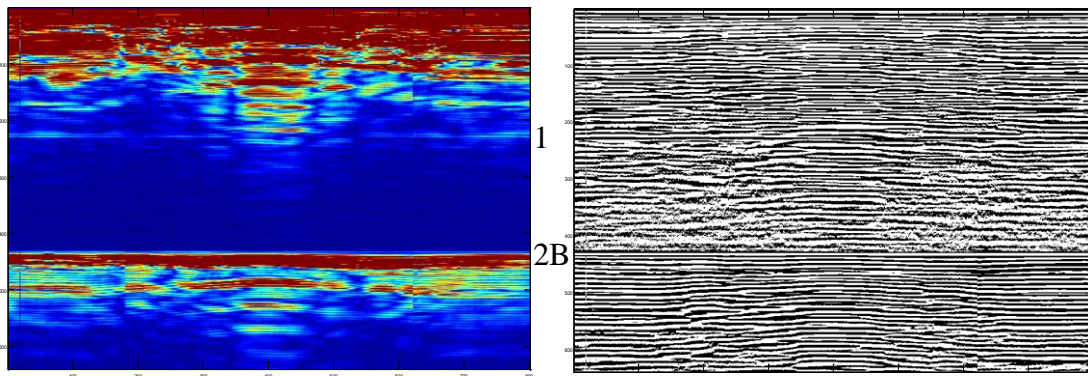

Figure 18: Instantaneous Amplitude (left) and "Instantaneous Phase" (right) at 5MHz of the specimen B and a 20 mm high stand-off.
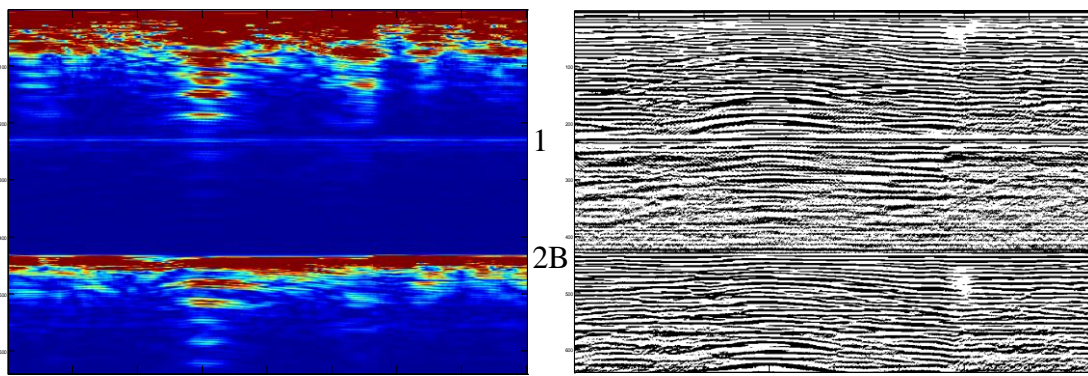

Figure 19: Instantaneous Amplitude (left) and "Instantaneous Phase" (right) at 5MHz of the specimen C and a 20 mm high stand-off.

The wrinkles are detectable in the three samples. The results for sample J (mainly UD carbon) were very promising and reproduce the results obtained with the FMC/TFM. The amplitude and the angle θ of the wrinkle are not measurable for samples B and C because there is no a clear ply-interface line to follow and the stand-off multiple echo appears across the wrinkle. If more time were available, a method that characterises the wrinkles in terms of the wrinkle angle[2] would be adequate. As in the TFM scans, only the top half of the part presents a clear image. The mainly carbon-fibre specimen (J) is easier to

12

characterise because the glass layers in B and C attenuate the signal, causing penetration to only half of the specimen or less.

Only the wrinkle in specimen J was characterised with both methods. For the OmniScan images, the measurement of the parameters were done with an electronic rule or protractor on the B-Scan slices reconstructed with Matlab. The results obtained are summarised in Table 4 and should be interpreted with reference to Figure 3.

Table 4: Comparison between the actual parameters of the parts and those obtained from the convex side of sample J.

	Expected	2.5 MHz probe with TFM	5 MHz probe with TFM	5 MHz probe with OmniScan
Wrinkle Maximum height H	3 mm	3.2 mm	3.5 mm	2.6 mm
Wrinkle "Severity" 2A/L	0.06	0.065	0.08	0.05
Wrinkle Angle θ	8.5°	8.5°	10°	7.6°

5. Conclusions

This paper shows that it is possible to use ultrasonic phased-array data for the detection and characterisation of out-of-plane wrinkles in complex glass/carbon- fibre composite materials. The FMC/TFM method presents, in general, better results whilst the phased-array technology introduced challenges that the FMC/TFM did not. The big dead zone with phased-array imposes the need for a stand-off to reduce the near-field depth of the beam in the laminate but then it is difficult focusing the beam – a larger aperture beam is required.

Further work is necessary to accurately determine the sensitivity of the technique. Also, the method for measuring the representative angle of the wrinkle is not the optimum, and a more systematic measurement of the angles for lines in the image[2] will be performed in the future. Finally, the velocity of the ultrasonic wave was considered constant in the full sample, while it is different for carbon and glass composites and for different angles. This effect, along with the effect of fibre volume fraction on velocity, may have influences on the wrinkle measurements that have yet to be considered.

Acknowledgements

References

1. H.M. Hsiao and I.M. Daniel, Effect of fiber waviness on stiffness and strength reduction of unidirectional composites under compressive loading, Composites Science and Technology, 56, (1996), 581-593.

2. R. A. Smith, L. J. Nelson, N. Xie, C. Fraij and S. R. Hallett, Progress in 3D characterisation and modelling of monolithic carbon-fibre composites, Insight, 57, 2015, pp. 131-139.

3. K. Mizukami, Y. Mizutami, K. Kimura, A. Sato, A. Todoroki, Y. Suzuki, Detection of in-plane waviness in cross-ply CFRP laminates using layer selectable eddy current method, Composites: Part A. 82 (2016) 108-118.

13

4. K. Mizukami, Y. Mizutami, K. Kimura, A. Sato, A. Todoroki, Y. Suzuki, Visualization and size estimation of fiber waviness in multidirectional CFRP laminates using eddy current imaging, Composites: Part A. 90 (2016) 261-270.

5. D. Pain, B. Drinkwater, Detection of fibre waviness using ultrasonic array scattering data, 18th world conference on Nondestructive Testing, 16-20 April 2012, Durban, South Africa.

6. R.A. Smith and B. Clarke, "Ultrasonic C-scan determination of ply stacking sequence in carbon-fibre composites," Insight - Journal of the British Institute of NDT, Vol. 36, No. 10,1994, pp. 741-747.

7. D. Hsu, D. Fei and Z. Liu, "Ultrasonically mapping the ply layup of composite laminates," Materials Evaluation, Vol 60 (9), 2002, pp 1099-1106.

8. R.A. Smith, L.J. Nelson, M.J. Mienczakowski and R.E. Challis, Automated Analysis and Advanced Defect Characterisation from Ultrasonic Scans of Composites, Insight – Non-Destructive Testing and Condition Monitoring, Vol 51, No 5, pp 82-87, 2009.

9. R. Smith, S. Hallett, P. Wilcox, L. Nelson, R. Tayong Boumda, N. Xie, and C. Fraij, Progress in non-destructive 3D characterization and modelling of aerospace composites, NDT of Composites II: Promoting Quality in Composite Inspection American Society of Nondestructive Testing (2015) pp. 38-44

10. C. Meola, S. Boccardi, G.M. Carlomagno, N.D. Boffa, E. Monaco, F. Ricci, Nondestructive evaluation of carbon fibre reinforced composites with infrared thermography and ultrasonics, Composites Structures 134 (2015) pp 845-853

11. K. Potter, B. Khan, M. Wisnom, T. Bell and J. Stevens, Variability, fibre waviness and misalignment in the determination of the properties of composite materials and structures, Composites: Part A. 39 (2008) 1343-1354.

12. D.O. Adams and S.J. Bell, Compression Strength reductions in composite laminates due to multiple-layer waviness, Composites Science and Technology 53 (1995) 207-212.

13. N. Xie, R.A. Smith, and S.R. Hallett, Parametric study of the effect of out-of-plane wrinkles on compressive strength of composites, (2016), (to be published)

14. L. J. Nelson and R. Smith, Three-dimensional fibre-orientation characterisation in monolithic carbon-fibre composites, 11th European Conference on Non-Destructive Testing (ECNDT 2014), October 6-10, 2014, Prague, Czech Republic

15. R. A. Smith, Use of 3D ultrasound data sets to map the localised properties of fibre-reinforced composites, PhD Thesis, University of Nottingham, July 2010.

16. R. A. Smith, L. J. Nelson, M. J. Mienczakowski and P. D. Wilcox. "Ultrasonic Tracking of Ply Drops in Composite Laminates." Proc. Review of Quantitative NDE, Minneapolis, July 2015, published in AIP Conference Proceedings 1706, 050006 (2016); doi: 10.1063/1.4940505, 2016.

17. C. Holmes, B. W. Drinkwater and P. D. Wilcox, "Post-processing of the full matrix of ultrasonic transmit-receive array data for non-destructive evaluation" NDT&E International 38, 2005, pp 701-711.

18. J. Zhang, B.W. Drinkwater, P.D. Wilcox, A. J. Hunter, "Defect detection using ultrasonic arrays: The multi-mode total focusing method", NDT&E International 43 2010, pp 123-133.

19. http://www.bris.ac.uk/engineering/research/ndt/research/array-imaging/

14